Inorg. Chem. **2008**, *47*, 6850−6862

Sterically Congested Uranyl Complexes with Seven-Coordination of the UO_2 Unit: the Peculiar Ligation Mode of Nitrate in $[UO_2(NO_3)_2(Rbtp)]$ Complexes†

Jean-Claude Berthet,*,‡ Pierre Thuéry,‡ Jean-Pierre Dognon,*,‡ Denis Guillaneux,§ and Michel Ephritikhine*,‡

Service de Chimie Moléculaire, DSM, IRAMIS, CNRS URA 331, CEA Saclay, 91191 Gif- sur-Yvette, France, and DEN/VRH/DRCP/SCPS/LCAM, CEA CE VALRHO, BP 17171, 30207 Bagnols-sur-Cèze, France

Received March 11, 2008

Addition of 1 or 2 molar equiv of Rbtp [Rbtp = 2,6-bis(5,6-dialkyl-1,2,4-triazin-3-yl)pyridine; R = Me, Pr^n] to $UO_2(OTf)_2$ in anhydrous acetonitrile gave the neutral compounds $[UO_2(OTf)_2(Rbtp)]$ [R = Me (**1**), ^{n}Pr (**2**)] and the cationic complexes $[UO_2(Rbtp)_2][OTf]_2$ [R = Me (**3**), Pr^n (**4**)], respectively. No equilibrium between the mono and bis(Rbtp) complexes or between $[UO_2(Rbtp)_2][OTf]_2$ and free Rbtp in acetonitrile was detected by NMR spectroscopy. The crystal structures of **1** and **3** resemble those of their terpyridine analogues, and **3** is another example of a uranyl complex with the uranium atom in the unusual rhombohedral environment. In the presence of 1 molar equiv of Rbtp in acetonitrile, $UO_2(NO_3)_2$ was in equilibrium with $[UO_2(NO_3)_2(Rbtp)]$ and the formation of the bis adduct was not observed, even with an excess of Rbtp. The X-ray crystal structures of $[UO_2(NO_3)_2(Rbtp)]$ [R = Me (**5**), Pr^n (**6**)] reveal a particular coordination geometry with seven coordinating atoms around the UO_2 fragment. The large steric crowding in the equatorial girdle forces the bidentate nitrate ligands to be almost perpendicular to the mean equatorial plane, inducing bending of the UO_2 fragment. The dinuclear oxo compound $[U(CyMe_4btbp)_2(\mu\text{-}O)UO_2(NO_3)_3][OTf]$ (**7**), which was obtained fortuitously from a 1:2:1 mixture of $U(OTf)_4$, $CyMe_4btbp$, and $UO_2(NO_3)_2$ [$CyMe_4btbp$ = 6,6′-bis-(3,3,6,6-tetramethyl-cyclohexane-1,2,4-triazin-3-yl)-2,2′-bipyridine] is a very rare example of a mixed valence complex involving covalently bound U^{IV} and U^{VI} ions; its crystal structure also exhibits a seven coordinate uranyl moiety, with one bidentate nitrate group almost parallel to the UO_2 fragment. The distinct structural features of $[UO_2(\kappa^2\text{-}NO_3)_2(Mebtp)]$, with its high coordination number and a noticeable bending of the UO_2 fragment, and of $[UO_2(\kappa^2\text{-}NO_3)(\kappa^1\text{-}NO_3)(terpy)]$, which displays a classical geometry, were analyzed by Density Functional Theory, considering the bonding energy components and the molecular orbitals involved in the interaction between the uranyl, nitrate, and Mebtp or terpy moieties. The unusual geometry of the Mebtp derivative with the seven coordinating atoms around the UO_2 fragment was found very stable. In both the Mebtp and terpy complexes, the origin of the interaction appears to be primarily steric (Pauli repulsion and electrostatic); this term represents 62−63% of the total bonding energy while the orbital term contributes to about 37−38%.

Introduction

The chemistry of uranyl compounds in anhydrous conditions is currently witnessing a spectacular development with the discovery of structural and chemical features which change the generally accepted ideas on the coordination geometry and the reactivity of the UO_2^{2+} ion.[1] The attention paid to the uranyl compounds is motivated by their exciting fundamental aspects and also by the aim of controlling their

† To the memory of Charles Madic.

* To whom correspondence should be addressed. E-mail: jean-claude.berthet@cea.fr (J.-C.B.), jean-pierre.dognon@cea.fr (J.-P.D.), michel.ephritikhine@cea.fr (M.E.).

‡ CEA Saclay.

§ CEA CE VALRHO.

(1) (a) Burns, C. J.; Eisen, M. S. In *The Chemistry of the Actinide and Transactinide Elements*, 3rd ed.; Morss, L. R., Edelstein, N., Fuger, J., Katz, J. J., Eds.; Springer: Dordrecht, The Netherlands, 2006; Vol. *5*, Chapter 25, p 2799. (b) Ephritikhine, M. *Dalton Trans.* **2006**, 2501.

10.1021/ic8004486 CCC: $40.75
Published on Web 06/27/2008

physicochemical properties and chemical behavior, this latter point being of particular importance in the nuclear industry and natural environment.[2]

Uranyl complexes were invariably found in the polygonal bipyramidal configuration with generally four or five and at the most six coordinating atoms lying in the equatorial plane perpendicular to the UO_2 fragment.[1] But recently, the use of sterically demanding bi- and terdentate nitrogen ligands in anhydrous media led to the formation of the six coordinate uranyl compounds $[Na(thf)_2(PhCN)_{0.5}][UO_2(NCN)_3]$ [NCN = $(Me_3SiN)_2CPh$],[3] $[UO_2(OTf)_2(bipy)_2]$, $[UO_2(phen)_3][OTf]_2$, and $[UO_2(terpy)_2][OTf]_2$,[4] in which the uranium atom is in a rhombohedral environment. The propeller-like shape of these complexes was exploited in the design strategy to obtain columnar phases for metallomesogens, by changing the phen ligand of $[UO_2(phen)_3][OTf]_2$ with an imidazo[4,5-f]-1;10-phenanthroline moiety bearing three long alkoxy chains.[5]

Following our studies on the complexation of the UO_2^{2+} ion with nitrogen aromatic bases (py, bipy, phen, and terpy),[4] we examined its behavior in the presence of the Rbtp and $CyMe_4$btbp molecules [Rbtp = 2,6-bis(5,6-dialkyl-1,2,4-triazin-3-yl)pyridine; $CyMe_4$btbp = 6,6′-bis-(3,3,6,6-tetramethyl-cyclohexane-1,2,4-triazin-3-yl)-2,2′-bipyridine]. These ter- and tetradentate ligands, represented in Scheme 1, are among the most efficient extractants in the selective complexation of trivalent actinide over lanthanide ions,[6] which is the basis of the SANEX process (Selective Actinide Extraction) for the partitioning of spent nuclear fuels.[7] In the prospect of the so-called GANEX process (for Group Actinide Extraction), which plans to reduce the number of extraction steps during the reprocessing,[8] it is desirable to have a better knowledge of the coordination chemistry of the actinide ions An^{n+} ($n = 3, 4$) and particularly the actinyl AnO_2^{n+} ($n = 1, 2$) ion with such polydentate nitrogen molecules. We have recently reported on crystal structures of the complexes $[UO_2(CyMe_4btbp)(py)][OTf]_2$, $[UO_2I$-

Scheme 1. Rbtp and $CyMe_4$btbp Ligands

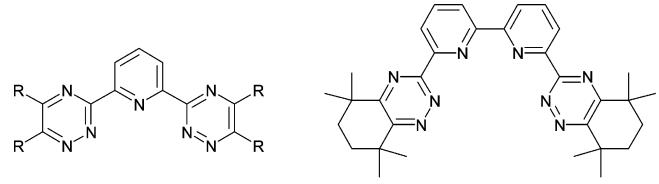

Rbtp $CyMe_4$btbp

$(CyMe_4btbp)][I]$, and some derivatives,[9] which exhibit the classical pentagonal bipyramidal configuration. Here we present the synthesis and structural characterization of a series of compounds resulting from the reactions of UO_2X_2 with Rbtp; the influence of X^- on the coordination of the terdentate ligand was considered by using two uranyl precursors with either weakly (X = OTf) or strongly (X = NO_3) coordinating counter-ions. Of special interest are the sterically congested nitrate derivatives $[UO_2(NO_3)_2(Rbtp)]$ (R = Me, Pr^n) which adopt a particular structure because of the presence of seven coordinating atoms around the UO_2 fragment, in contrast to the terpyridine analogue $[UO_2(NO_3)_2(terpy)]$ which was found in the classical hexagonal bipyramidal configuration.[10] This peculiar coordination geometry was also found in the $[U^{IV}U^{VI}]$ mixed valence oxo complex $[U(CyMe_4btbp)_2(\mu\text{-}O)UO_2(\kappa^2\text{-}NO_3)_3][OTf]$ which was obtained fortuitously from a 1:1:2 mixture of $U(OTf)_4$, $UO_2(NO_3)_2$, and $CyMe_4$btbp. The non classical structural features of $[UO_2(\kappa^2\text{-}NO_3)_2(Rbtp)]$ in contrast to the typical structure of the terpy derivative $[UO_2(\kappa^2\text{-}NO_3)(\kappa^1\text{-}NO_3)(terpy)]$ are discussed in light of theoretical calculations on the $[UO_2(NO_3)_2(L)]$ complexes (L = Mebtp, terpy), with a detailed analysis of their energy and geometries, and of the interactions between the uranyl, nitrate, and terdentate nitrogen ligands.

Experimental Section

All reactions were carried out under argon (<5 ppm oxygen or water) using standard Schlenk-vessel and vacuum line techniques or in a glovebox. Solvents were dried by standard methods and distilled immediately before use; deuterated acetonitrile (Eurisotop) was distilled over Na/K alloy and stored over 3 Å molecular sieves. IR samples were prepared as Nujol mulls between KBr round cell windows, and the spectra recorded on a Perkin-Elmer FT-IR 1725X spectrometer. The ^1H NMR spectra were recorded on a Bruker DPX 200 instrument and referenced internally using the residual protio solvent resonances relative to tetramethylsilane (δ 0). Elemental analyses were performed by Analytische Laboratorien at Lindlar (Germany).

Caution! *In addition to the radioactive hazards of uranium, this metal is chemically toxic and must be handled with care, following appropriate procedures.*

Syntheses. Mebtp, Pr^nbtp,[11] $U(OTf)_4$,[12] and $UO_2(OTf)_2$[13] were prepared by a published method; $[UO_2(NO_3)_2(MeCN)]$ was obtained

(2) (a) Dam, H. H.; Beijleveld, H.; Reinhoudt, D. N.; Verboom, W. *J. Am. Chem. Soc.* **2008**, *130*, 5542. (b) Dam, H. H.; Reinhoudt, D. N.; Verboom, W. *Chem. Soc. Rev.* **2007**, *36*, 367. (c) Gorden, A. E. V.; Xu, J.; Raymond, K. N.; Durbin, P. *Chem. Rev.* **2003**, *103*, 4207. (d) Andreev, G. B.; Budantseva, N. A.; Fedoseev, A. M. In *Structural Chemistry of Inorganic Actinide Compounds*; Krivovichev, S. V., Burns, P. C. I. G., Tananaev, I. G., Eds.; Elsevier: London, 2007; Chapter 10, p 363.
(3) Sarsfield, M. J.; Helliwell, M.; Raftery, J. *Inorg. Chem.* **2004**, *43*, 3170.
(4) Berthet, J. C.; Nierlich, M.; Ephritikhine, M. *Dalton Trans.* **2004**, 2814.
(5) Cardinaels, T.; Ramaekers, J.; Guillon, D.; Donnio, B.; Binnemans, K. *J. Am. Chem. Soc.* **2005**, *127*, 17602.
(6) Berthet, J. C.; Miquel, Y.; Iveson, P. B.; Nierlich, M.; Thuéry, P.; Madic, C.; Ephritikhine, M. *J. Chem. Soc., Dalton Trans.* **2002**, 3265.
(7) (a) Actinides and Fission Products Partitioning and Transmutation. Status and Assessment Report, NEA/OECD Report, NEA/OECD, Paris, 1999. (b) Actinides and Fission Products Partitioning and Transmutation. Proceedings of the Fifth International Information Exchange Meeting, Mol, Belgium, 25−27 Nov. 1998, NEA/OECD Report, NEA/OECD, Paris, 1999. (c) Nash, K. L.; Madic, C.; Mathur, J. N. Lacquement, J. In *The Chemistry of the Actinide and Transactinide Elements*, 3rd ed.; Morss, L. R., Edelstein, N., Fuger, J., Katz, J. J., Eds.; Springer: Dordrecht, The Netherlands, 2006; Vol. *4*, Chapter 24, p 2622.
(8) (a) Mirguiditchian, M.; Chareyre, L.; Technical Report CEA/DRCP/SCPS/2006/12, CEA DEN, Bagnols-sur-Cèze, 2006. (b) Mirguiditchian, M.; Technical report CEA/DRCP/SCPS/2004/31, CEA DEN, Bagnols-sur-Cèze, 2004.
(9) Berthet, J. C.; Thuéry, P.; Foreman, M. R. StJ.; Ephritikhine, M. *Radiochim. Acta* **2008**, *96*, 189.
(10) Charushnikova, I. A.; Den Auwer, C. *Russ. J. Coord. Chem.* **2004**, *30*, 511.
(11) (a) Drew, M. G. B.; Guillaneux, D.; Hudson, M. J.; Iveson, P. B.; Russell, M. L.; Madic, C. *Inorg. Chem. Commun.* **2001**, *4*, 12. (b) Case, F. H. *J. Heterocycl. Chem.* **1971**, *8*, 1043.

by refluxing an acetonitrile solution of $UO_2(NO_3)_2 \cdot 6H_2O$ in a Kumagawa (analogous to Soxhlet) apparatus for 1 week, the water molecules being trapped by the molecular sieves (4 Å) placed on the fritted filter.

$[UO_2(OTf)_2(Mebtp)]$ (1). A flask was charged with $UO_2(OTf)_2$ (10 mg, 0.017 mmol) and Mebtp (5.1 mg, 0.017 mmol) in acetonitrile (0.5 mL). Addition of Et_2O (2 mL) induced the precipitation of the beige powder of **1** which was filtered off and dried under vacuum. Yield: 13.6 mg (90%). ^{1}H NMR (acetonitrile-d_3, 23 °C): δ 9.47 (d, J = 8.1 Hz, 2H, *m*-H), 8.98 (t, J = 8.1 Hz, 1 H, *p*-H,), 3.15 and 3.04 (s, 2 × 6H, Me). IR (nujol): ν/cm^{-1} 1549s, 1392m, 1339s, 1273ws, 1236m, 1185vs, 1084w, 1009w, 987s, 947s [ν_{asym} (U=O)], 871w, 851w, 796m, 782w, 630s. Pale yellow crystals of **1**·0.5MeCN suitable for X-ray diffraction analysis were grown by slow diffusion of diethyl ether into an acetonitrile solution of **1**.

$[UO_2(OTf)_2(Pr^nbtp)]$ (2). A flask was charged with $UO_2(OTf)_2$ (82.5 mg, 0.14 mmol) and Pr^{n}btp (58.9 mg, 0.14 mmol) and acetonitrile (5 mL) was condensed in it. After stirring for 90 min at 20 °C, the volume of the pale yellow solution was reduced by evaporation to about 2 mL and addition of Et_2O (5 mL) led to the precipitation of a yellow powder of **2** which was filtered off and dried under vacuum. Yield: 96 mg (68%). Anal. Calcd. for $C_{25}H_{31}N_7O_8F_6S_2U$: C, 30.84; H, 3.21; N, 10.07. Found: C, 30.81; H, 3.21; N, 10.18. ^{1}H NMR (acetonitrile-d_3, 23 °C): δ 9.50 (d, J = 7.8 Hz, 2 H, *m*-H), 8.98 (t, J = 7.8 Hz, 1 H, *p*-H), 3.46 and 3.34 (t, J = 7.3 Hz, 2 × 4H, $MeCH_2CH_2$), 2.16 (m, 8 H, $MeCH_2CH_2$), 1.26 and 1.25 (t, J = 7.5 Hz, 2 × 6H, Me). IR (nujol): ν/cm^{-1} 1603m, 1537vs, 1332vs, 1236m, 1185vs, 1161s, 1086w, 1006vs, 987vs, 946vs [ν_{asym} (U=O)], 863w, 847s, 789w, 631vs, 588m, 570w, 511s.

$[UO_2(Mebtp)_2][OTf]_2$ (3). An NMR tube was charged with $UO_2(OTf)_2$ (20 mg, 0.035 mmol) and Mebtp (20.6 mg, 0.070 mmol) in acetonitrile-d_3 (0.5 mL). After 5 min at 80 °C, the pale orange solution was evaporated to dryness and the white cream powder of **3** was obtained after washing with tetrahydrofuran (thf, 1 mL) and drying under vacuum. Yield: 37 mg (91%). Anal. Calcd. for $UO_8C_{32}F_6S_2N_{14}H_{30}$: C, 33.28; H, 2.61; N, 16.98. Found: C, 32.85; H, 2.76; N, 16.72. ^{1}H NMR (acetonitrile-d_3, 23 °C): δ 9.38 (d, J = 7.9 Hz, 2 H, *m*-H), 8.97 (t, J = 7.9 Hz, 1 H, *p*-H), 3.04 and 2.65 (s, 2 × 6 H, Me). IR (nujol): ν/cm^{-1} 1552m, 1526m, 1394m, 1312w, 1264vs (OTf), 1223m, 1150vs, 1079m, 1025s, 941vs [ν_{asym}(U=O)], 842m, 794m, 778m, 725m, 632vs, 572w, 516m. Almost colorless crystals of **3**·2MeCN suitable for X-ray diffraction analysis were grown by slow diffusion of diethyl ether into a 1:1 mixture of $UO_2(OTf)_2$ and Mebtp in acetonitrile.

$[UO_2(Pr^nbtp)_2][OTf]_2$ (4). An NMR tube was charged with $UO_2(OTf)_2$ (15.4 mg, 0.027 mmol) and Pr^{n}btp (22.0 mg, 0.054 mmol) in acetonitrile-d_3 (0.5 mL). After 5 min at 80 °C, the pale orange solution was evaporated to dryness, the residue was dissolved in thf (0.5 mL), and Et_2O (0.5 mL) was condensed into this solution. The suspension was heated at about 50 °C, giving a clear yellow-orange solution from which pale yellow crystals of **4** were deposited in a few hours upon slow cooling to room temperature; Yield: 26.5 mg (71%). Calcd. for $UO_8C_{48}F_6S_2N_{14}H_{62}$: C, 41.80; H, 4.53; N, 14.21. Found: C, 41.86; H, 4.42; N, 13.82. ^{1}H NMR (acetonitrile-d_3, 23 °C): δ 9.42 (d, J = 7.9 Hz, 2 H, *m*-H), 8.98 (t, J = 7.9 Hz, 1 H, *p*-H), 3.25 and 2.94 (t, J = 7.4 Hz, 2 × 4 H, $MeCH_2CH_2$), 2.20 and 1.36 (hex, J = 7.4 Hz, 2 × 4 H, $MeCH_2CH_2$), 1.33 and 0.92 (t, J = 7.4 Hz, 2 × 6 H, Me). IR (nujol): ν/cm^{-1} 1599w, 1574w, 1535s, 1313w, 1261vs (OTf), 1222m, 1148vs, 1079s, 1029s, 1008m, 991w, 942s [ν_{asym} (U=O)], 845w, 822w, 781w, 741s, 636vs, 571m, 516m.

$[UO_2(NO_3)_2(Mebtp)]$ (5). A flask was charged with $[UO_2(NO_3)_2(MeCN)]$ (53.7 mg, 0.12 mmol) and Mebtp (33.8 mg, 0.11 mmol) and acetonitrile (5 mL) was condensed in it. After stirring for 15 min at 20 °C, the pale yellow solution was filtered and evaporated off, and the yellow residue was washed with thf (4 mL). The yellow powder of **5** was obtained after drying under vacuum. Yield: 51 mg (64%). Calcd. for $C_{15}H_{15}N_9O_8U$: C, 26.21; H, 2.20; N, 18.34; Found: C, 25.88; H, 2.14; N, 18.40. ^{1}H NMR (acetonitrile-d_3, 23 °C): δ 9.39 (br, $w_{1/2}$ = 23 Hz, 2 H, *m*-H), 8.87 (t, $w_{1/2}$ = 23 Hz, 1 H, *p*-H), 2.96 (s, $w_{1/2}$ = 17 Hz, 12 H, Me). The spectrum at −20 °C shows well resolved signals of **5** and the free ligand which are in relative proportions of about 75:25; ^{1}H NMR (acetonitrile-d_3, −20 °C): δ 9.38 (d, J = 7.8 Hz, 2 H, *m*-H), 8.87 (t, J = 7.8 Hz, 1 H, *p*-H), 2.98 and 2.93 (s, 2 × 6 H, Me); δ_H for free Mebtp: 8.66 (d, J = 7.8 Hz, 2 H, *m*-H), 8.20 (t, J = 7.8 Hz, 1 H, *p*-H), 2.98 and 2.93 (s, 2 × 6 H, Me). IR (nujol): ν/cm^{-1} 1554s, 1486 m, 1286vs, 1091m, 1079m, 1000s, 939vs [ν_{asym} (U=O)], 842w, 922w, 802m, 779m, 641w, 613w. Slow diffusion of diethyl ether into a 1:1 or 1:2 mixture of $UO_2(NO_3)_2(MeCN)$ and Mebtp in acetonitrile led to the formation of yellow crystals of **5**·MeCN.

$[UO_2(NO_3)_2(Pr^nbtp)]$ (6). A flask was charged with $[UO_2(NO_3)_2(MeCN)]$ (33.9 mg, 0.078 mmol) and Pr^{n}btp (28.6 mg, 0.070 mmol), and acetonitrile (5 mL) was condensed in it. The suspension was heated under reflux in a sand bath at 110 °C, giving a gold-yellow solution from which a yellow powder was deposited upon cooling down to 25 °C. The volume of the solution was reduced to about 2 mL, and the yellow powder of **6** was filtered off, washed with a 3:1 mixture of Et_2O and thf (4 mL), and dried under vacuum. Yield: 31 mg (55%). Calcd. for $C_{23}H_{31}N_9O_8U$: C, 34.55; H, 3.90; N, 15.76. Found: C, 34.36; H, 3.74; N, 15.68. ^{1}H NMR (acetonitrile-d_3, 23 °C): δ 9.45 (br, $w_{1/2}$ = 10 Hz, 2 H, *m*-H), 8.89 (br, $w_{1/2}$ = 20 Hz, 1 H, *p*-H), 3.25 (br, $w_{1/2}$ = 30 Hz, 8 H, $MeCH_2CH_2$), 2.15 (m, $w_{1/2}$ = 30 Hz, 8 H, $MeCH_2CH_2$), 1.23 (t, J = 7 Hz, 12 H, Me). The low-temperature spectra exhibit the signals of **6** and free Pr^{n}btp, in variable proportions depending on the crystallization of the products. ^{1}H NMR (acetonitrile-d_3, −20 °C): δ 9.46 (d, J = 7.8 Hz, 2 H, *m*-H), 8.89 (t, J = 7.8 Hz, 1 H, *p*-H), 3.27 and 3.20 (t, J = 7.5 Hz, 2 × 4 H, $MeCH_2CH_2$), 2.11 (m, partially masked by the solvent, $MeCH_2CH_2$, 8 H), 1.18 (t, J = 7.5 Hz, 12 H, Me); δ_H for free Pr^{n}btp: 8.62 (d, J = 7.8 Hz, 2 H, *m*-H), 8.18 (t, J = 7.8 Hz, 1 H, *p*-H), 2.97 and 2.89 (t, J = 7.6 Hz, 2 × 4 H, $MeCH_2CH_2$), 1.85 (m, partially masked by the solvent, $MeCH_2CH_2$, 8H), 1.06 (t, J = 7.5 Hz, 12 H, Me). IR (nujol): ν/cm^{-1} 1546m, 1492m, 1286s, 1249m, 1153w, 1088w, 1066w, 1024w, 1011w, 916s [ν_{asym} (U=O)], 844w, 810w, 777w. An NMR tube was charged with $UO_2(NO_3)_2(MeCN)$ (10.0 mg, 0.023 mmol) and Pr^{n}btp (9.0 mg, 0.023 mmol) in acetonitrile (0.5 mL). After heating under reflux, slow cooling of the gold-yellow solution down to room temperature induced the formation of yellow-orange crystals of **6**.

Crystals of $[U(CyMe_4btbp)_2(\mu\text{-}O)UO_2(\kappa^2\text{-}NO_3)_3][OTf]\cdot 2MeCN$ (7·2MeCN). An NMR tube was charged with $U(OTf)_4$ (10.0 mg, 12 mmol), $CyMe_4$btbp (12.8 mg, 12 mmol), and $[UO_2(NO_3)_2(MeCN)]$ (5.2 mg, 12 mmol) in acetonitrile (0.5 mL). Slow diffusion of diethyl ether into the orange solution led, after 1 month at 19 °C, to the formation of small dark orange crystals of **7**·2MeCN.

(12) Berthet, J. C.; Lance, M.; Nierlich, M.; Ephritikhine, M. *Eur. J. Inorg. Chem.* **1999**, 2005.
(13) Berthet, J. C.; Lance, M.; Nierlich, M.; Ephritikhine, M. *Eur. J. Inorg. Chem.* **2000**, 1969.

Table 1. Crystal Data and Structure Refinement Details

	1·0.5MeCN	**3**·2MeCN	**5**·MeCN	**6**	**7**·2MeCN
chemical formula	$C_{18}H_{16.5}F_6N_{7.5}O_8S_2U$	$C_{36}H_{36}F_6N_{16}O_8S_2U$	$C_{17}H_{18}N_{10}O_8U$	$C_{23}H_{31}N_9O_8U$	$C_{69}H_{82}F_3N_{21}O_{15}SU_2$
M/g mol^{-1}	882.04	1236.96	728.44	799.60	2010.68
crystal system	monoclinic	monoclinic	triclinic	monoclinic	monoclinic
space group	$P2_1/n$	$P2/c$	$P\bar{1}$	$P2_1/c$	$P2_1/n$
a/Å	14.3757(6)	31.543(2)	8.7996(4)	10.6725(2)	16.6734(8)
b/Å	25.5931(16)	6.2642(2)	9.2294(5)	17.9793(7)	29.3252(17)
c/Å	15.2088(10)	25.3392(17)	15.5220(9)	15.3329(6)	18.0981(8)
α/°	90	90	104.861(3)	90	90
β/°	100.700(4)	111.379(3)	98.721(2)	98.485(2)	116.311(3)
γ/°	90	90	102.410(3)	90	90
V/Å^3	5498.3(6)	4662.3(5)	1161.09(11)	2909.94(17)	7932.3(7)
Z	8	4	2	4	4
D_{calc}/g cm^{-3}	2.131	1.762	2.084	1.825	1.684
μ (Mo Kα)/mm^{-1}	6.154	3.662	7.056	5.639	4.187
F(000)	3352	2424	692	1552	3960
temperature/K	100(2)	100(2)	100(2)	200(2)	100(2)
reflections collected	216606	132752	44575	93394	201334
independent reflections	10407	8867	4403	5508	15037
observed reflections [$I > 2\sigma(I)$]	8973	4908	4280	4696	10137
R_{int}	0.038	0.044	0.037	0.022	0.066
parameters refined	775	635	330	411	1018
$R1$	0.036	0.035	0.017	0.027	0.062
$wR2$	0.093	0.088	0.043	0.068	0.159
S	1.047	0.990	1.047	1.073	1.024
$\Delta\rho_{min}$/e Å^{-3}	−0.99	−1.16	−1.00	−1.02	−0.93
$\Delta\rho_{max}$/e Å^{-3}	1.99	1.01	0.48	1.18	2.29

Crystallographic Data Collection and Structure Determination. The data were collected on a Nonius Kappa-CCD area detector diffractometer[14] using graphite-monochromated Mo Kα radiation (λ 0.71073 Å).The crystals were introduced in glass capillaries with a protecting "Paratone-N" oil (Hampton Research) coating. The unit cell parameters were determined from ten frames, then refined on all data. The data (combinations of φ- and ω-scans giving complete data sets up to $\theta = 25.7°$ and a minimum redundancy of 4 for 90% of the reflections) were processed with HKL2000.[15] The structures were solved by direct methods (**1**·0.5MeCN, **3**·2MeCN, and **6**) or Patterson map interpretation (**5**·MeCN and **7**·2MeCN) with SHELXS-97 and subsequent Fourier-difference synthesis and refined by full-matrix least-squares on F^2 with SHELXL-97.[16] Absorption effects were corrected empirically with the program SCALEPACK.[15] All non-hydrogen atoms were refined with anisotropic displacement parameters. The hydrogen atoms were introduced at calculated positions and were treated as riding atoms with a displacement parameter equal to 1.2 (CH, CH_2) or 1.5 (CH_3) times that of the parent atom. The data for compound **6** were recorded at 200(2) K since the crystals deteriorated at 100(2) K; in this compound, one nitrate ion is disordered over two positions which have been refined with occupancy parameters constrained to sum to unity and restraints on displacement parameters (restraints were also applied for some atoms of the propyl chains).

Crystal data and structure refinement parameters are given in Table 1. The molecular plots were drawn with SHELXTL[17] and Balls & Sticks.[18]

Computational Details. DFT (Density Functional Theory) calculations were performed with the Amsterdam Density Functional (ADF) program[19] (version 2007.01) using the Perdew−Burke−Ernzerhof (PBE) generalized-gradient approximation exchange correlation functional.[20] Scalar relativistic corrections were included via the ZORA model.[21] TZ2P ZORA all-electrons basis sets (relativistic valence triple-ζ with 2 polarization functions) were used for all atoms. One may notice that these are not trivial calculations, with 324 electrons, 1132 Slater Fragments Orbitals and inclusion of scalar relativistic effects.

Usually, DFT methods produce a reasonable geometry but they can present some difficulties for ion molecule interactions with, in some cases, poor accuracy for energy calculations.[22] To check the absence of troubles and establish the results, MP2 energy calculations on DFT optimized geometries were performed using the TURBOMOLE 5.9.1 program package[23] with the polarized split-valence SVP basis set and the 60-core electrons effective core potential of Cao and Dolg.[24]

The ADF energy decomposition scheme was used to analyze the electronic structure and the bonding properties in the complexes. The bonding energy analysis is performed combining a fragment approach to the molecular structure of chemical systems with the total bonding energy decomposition in electrostatic, Pauli repulsion, and orbital mixing terms. A detailed description of the physical significance of these terms has been given by Bickelhaupt and Baerends.[25] The Voronoi Deformation Density (VDD) charges[26] were calculated to evaluate the charge rearrangements due to the formation of the complex from the uranyl, nitrate, and Mebtp or terpy fragments. The VDD calculates the flow of electron

(14) *Kappa-CCD Software*; Nonius B.V.: Delft, The Netherlands, 1998.
(15) Otwinowski, Z.; Minor, W. *Methods Enzymol.* **1997**, *276*, 307.
(16) Sheldrick, G. M. *SHELXS-97 and SHELXL-97*; University of Göttingen: Göttingen, Germany, 1997.
(17) Sheldrick, G. M. *SHELXTL*, Version 5.1; Bruker AXS Inc.: Madison, WI, 1999.
(18) Ozawa, T. C.; Kang, S. J. *J. Appl. Crystallogr.* **2004**, *37*, 679.
(19) *ADF2007.01*; SCM, Theoretical Chemistry, Vrije Universiteit: Amsterdam, The Netherlands; http://www.scm.com.
(20) Perdew, J. P.; Burke, K.; Ernzerhof, M. *Phys. Rev. Lett.* **1996**, *77*, 3865.
(21) van Lenthe, E.; Baerends, E. J.; Snijders, J. G. *J. Chem. Phys.* **1993**, *99*, 4597.
(22) Gutowski, K. E.; Cocalia, V. A.; Griffin, S. T.; Bridges, N. J.; Dixon, D. A.; Rogers, R. D. *J. Am. Chem. Soc.* **2007**, *129*, 526.
(23) Ahlrichs, R.; Bär, M.; Häser, M.; Horn, H.; Kölmel, C. *Chem. Phys. Lett.* **1989**, *162*, 165; for current version, see http://www.turbomole.com.
(24) Cao, X.; Dolg, M. *J. Mol. Struct.* **2004**, *673*, 203.

density to or from a certain atom or fragment as a result of bond formation or charge rearrangements. This method does not explicitly use the basis functions. The Mayer Bond Orders[27] were also calculated. The participation from a specific orbital to a molecular orbital is obtained from a symmetrized fragment orbital analysis (see G. Te Velde et al. for details[28]).

Results and Discussion

Synthesis and Characterization of the Triflate Complexes. Treatment of $UO_2(OTf)_2$ with 1 or 2 molar equiv of Rbtp in acetonitrile led to the immediate and quantitative formation of $[UO_2(OTf)_2(Rbtp)]$ [R = Me (**1**), Pr^n (**2**)] or $[UO_2(Rbtp)_2][OTf]_2$ [R = Me (**3**), R = Pr^n (**4**)], respectively. These syntheses are similar to those of the neutral and cationic terpyridine analogues $[UO_2(OTf)_2(terpy)]$ and $[UO_2(terpy)_2][OTf]_2$ in pyridine or acetonitrile.[4] The ^{1}H NMR spectra of **1**−**4** are well resolved, and no equilibrium was detected at 23 °C between the mono- and bis-adducts **1** and **3** (or **2** and **4**) or between the complexes and free Rbtp. After evaporation of acetonitrile, compounds **1** and **2** were isolated as a beige and pale yellow powder in 90 and 68% yield, respectively; the white cream powder of **3** was obtained in 91% yield after washing with thf, whereas the light yellow microcrystalline powder of **4** was deposited in 71% yield from a cooled thf-Et_2O solution. Crystals of **1**·0.5MeCN and **3**·2MeCN suitable for X-ray diffraction analysis were grown by slow diffusion of diethyl ether into an acetonitrile solution of **1** and **3**.

The IR spectra of compounds **1**−**4** as Nujol mulls exhibit the peaks characteristic of the UO_2 asymmetric stretching mode at 947, 946, 941, and 942 cm^{-1}, respectively.[4] These values for the mono and bis(Mebtp) compounds are slightly larger than those of the corresponding terpyridine counterparts $[UO_2(OTf)_2(terpy)]$ (945 cm^{-1}) and $[UO_2(terpy)_2][OTf]_2$ (933 cm^{-1}),[4] in agreement with the weaker Lewis basicity of Rbtp. The spectra of **1** and **2** also show strong vibrations at 1338 and 1330 cm^{-1}, respectively, attributed to monodentate triflate ligands.[29]

X-ray Crystal Structures of the Triflate Complexes $[UO_2(OTf)_2(Rbtp)]$ [R = Me (1), ^{n}Pr (2)] and $[UO_2(Mebtp)_2][OTf]_2$ (3). The crystals of **1**·0.5MeCN contain two independent molecules in the asymmetric unit, labeled A and B, which differ by the position of the monodentate triflate ligands. Views of molecule A are shown in Figure 1a,b while selected bond lengths and angles are listed in Table 2; in the following, the values for molecule B are given in brackets. The complex adopts the classical pentagonal bipyramidal configuration whose characteristics can be compared with those of the terpy derivative $[UO_2(OTf)_2(terpy)]$ (Table 3). The U, N(1), N(3), N(6), O(3), O(6)

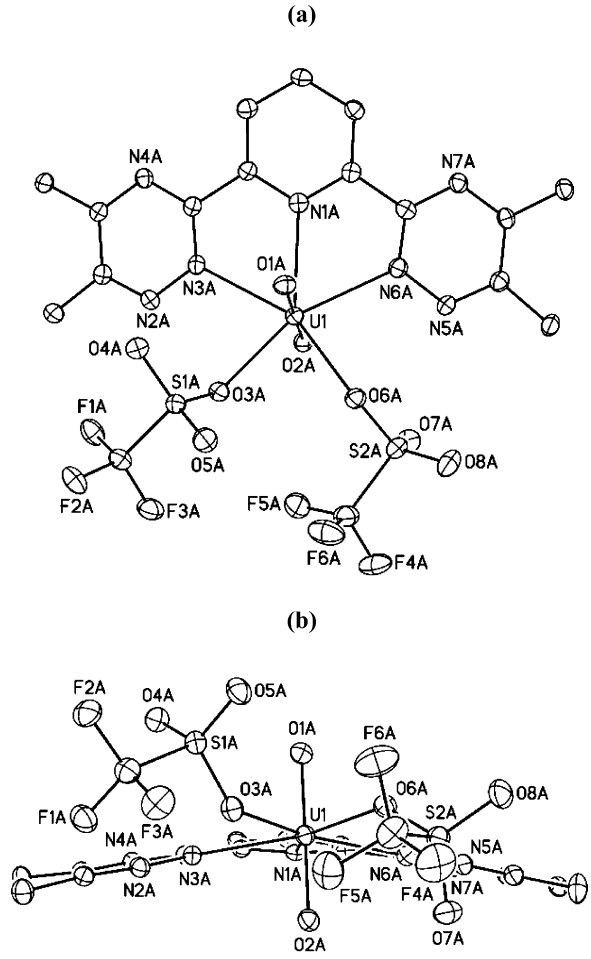

Figure 1. Views of one of the two independent molecules in $[UO_2(OTf)_2(Mebtp)]$ (**2**) along (a) and perpendicular to (b) the UO_2 axis. The hydrogen atoms have been omitted. The displacement ellipsoids are drawn at the 30% probability level.

atoms in **1** define the equatorial plane, and the maximum deviations from this plane are those of N(1A) and N(1B) which are 0.1 Å smaller than that of the central nitrogen atom of the terdentate ligand in $[UO_2(OTf)_2(terpy)]$. Considering only the aromatic rings, the Mebtp ligand is planar with an rms deviation of 0.17 [0.20] Å, being thus much less distorted than terpy in $[UO_2(OTf)_2(terpy)]$ (Table 3). This may be attributed to the withdrawing effect of the lateral triazine groups which favor a stronger electron delocalization inside the Rbtp molecule, thus inducing greater planarity. The lateral triazine rings form dihedral angles with the central pyridine ring which are smaller than those between the lateral and central pyridine rings in the terpy analogue. The U=O distances in the linear UO_2 fragment are classical. The mean U−O(OTf) bond length of 2.351(7) Å is identical to that measured in $[UO_2(OTf)_2(terpy)]$ [2.354(1) Å] and is close to those determined in $[UO_2(OTf)_2(py)_3]$ [2.370(2) and 2.394 (2) Å].[13] The U−N(btp) distances which average 2.57(2) Å seem larger than the mean U−N(terpy) distance of 2.541(8) Å in $[UO_2(OTf)_2(terpy)]$; the central U−N bond is slightly longer than the two lateral U−N bonds in **1** while practically no difference was observed between the three U−N bond lengths in $[UO_2(OTf)_2(terpy)]$. These structural features, if significant, would reflect the lesser affinity of Mebtp, in

(25) Bickelhaupt, F. M.; Baerends, E. J. In *Rev. Comput. Chem.*; Lipkowitz, K. B., Boyd, D. B., Eds.; Wiley-VCH: New York, 2000; Vol. 15, p 1.
(26) Fonseca Guerra, C.; Handgraaf, J. W.; Baerends, E. J.; Bickelhaupt, F. M. *J. Comput. Chem.* **2004**, *25*, 189.
(27) Mayer, I. *Chem. Phys. Lett.* **1983**, *97*, 270.
(28) Te Velde, G.; Bickelhaupt, F. M.; van Gisbergen, S. J. A.; Fonseca Guerra, C.; Baerends, E. J.; Snijders, J. G.; Ziegler, T. *J. Comput. Chem.* **2001**, *22*, 931.
(29) Lawrance, G. A. *Chem. Rev.* **1986**, *86*, 17.

Table 2. Selected Distances (Å) and Angles (deg) in the Triflate Uranyl Complexes

$[UO_2(OTf)_2(Mebtp)]$ in **1**·0.5MeCN[a]	$[UO_2(Mebtp)_2]^{2+}$ in **3**·2MeCN[a]
U(1)−O(1A) 1.760(4) [1.759(4)]	U(1)−O(1A) 1.759(4) [1.756(4)]
U(1)−O(2A) 1.755(4) [1.750(4)]	
U(1)−N(1A) 2.595(5) [2.588(5)]	U(1)−N(1A) 2.612(4) [2.591(4)]
U(1)−N(3A) 2.582(5) [2.579(5)]	U(1)−N(3A) 2.559(4) [2.560(4)]
U(1)−N(6A) 2.539(5) [2.545(5)]	U(1)−N(6A) 2.576(5) [2.567(4)]
U(1)−O(3A) 2.354(4) [2.359(4)]	
U(1)−O(6A) 2.351(4) [2.340(4)]	
O(1A)−U(1)−O(2A) 178.03(18) [177.62(18)]	O(1)−U(1)−O(1′)[b] 180 [180]
N(1A)−U(1)−N(3A) 61.91(15) [62.24(14)]	N(1A)−U(1)−N(3A) 60.37(14) [60.24(13)]
N(1A)−U(1)−N(6A) 62.16(15) [61.88(14)]	N(1A)−U(1)−N(6A) 60.11(14) [60.47(13)]
N(3A)−U(1)−O(3A) 77.69(14) [76.28(14)]	N(3A)−U(1)−N(6A′) 67.30(15) [67.15(14)]
N(6A)−U(1)−O(6A) 81.96(14) [80.05(14)]	
O(3A)−U(1)-O(6A) 77.60(13) [80.69(13)]	

[a] The corresponding values for the second independent molecule are given in square brackets. [b] Symmetry code: ′ = 1 − *x*, −*y*, 2 − *z* in molecule A; −*x*, 2 − *y*, −*z* in molecule B.

comparison with terpy, for $UO_2(OTf)_2$, in line with its weaker Lewis basicity. A reverse order was clearly observed between the trivalent complexes $[U(Pr^nbtp)_3]^{3+}$ and $[U(terpy)_3]^{3+}$ where the shorter U−N(Rbtp) distances reflect the stronger affinity in solution of the Rbtp versus terpy ligands; in that case, the distinct behavior of the two terdentate ligands was explained by the presence of a π back-bonding interaction between the U(III) ion and the aromatic nitrogen ligand, which is stronger with the more π accepting Rbtp molecule.[30]

Views of one of the two independent and centrosymmetric $[UO_2(Mebtp)_2]^{2+}$ cations of complex **3**·2MeCN are shown in Figure 2a,b, and selected bond lengths and angles are listed in Table 2. The structure resembles that of the terpy analogue $[UO_2(terpy)_2]^{2+}$, providing a new example of an uranyl complex in a rhombohedral configuration. The two parallel and staggered equilateral triangles N(1)N(3′)N(6′) and N(1′)N(3)N(6) are separated by 0.840(5) Å in complexes A and B; the UO_2 axis is perpendicular to these triangles, passing through their center, and the U atom, because of the imposed symmetry, is equidistant from the two planes. The U=O and U−N distances of both complexes A and B in **3** average 1.7575(15) and 2.58(2) Å, respectively, and are identical to those measured in the terpy counterpart $[UO_2(terpy)_2][OTf]_2$ [1.759(2) and 2.58(1) Å]. However, as observed above with the structures of $[UO_2(OTf)_2(Mebtp)]$ (**1**) and $[UO_2(OTf)_2(terpy)]$, comparison of the structures of **3** and its terpy analogue (Table 3) shows that the Mebtp ligand is less distorted than terpy; in **1**, the central U−N distances are larger than the lateral U−N distances while these distances are practically equal in the terpy derivative.

Synthesis and Characterization of the Nitrate Complexes. The bright yellow nitrate complexes $[UO_2(NO_3)_2(Rbtp)]$ [R = Me (**5**), Pr^n (**6**)] were synthesized from a 1:1 mixture of $UO_2(NO_3)_2(MeCN)$ and Rbtp in acetonitrile. These complexes are less soluble than their triflate counterparts **1** and **2**. Although ^{n}Prbtp has a much greater solubility than Mebtp in MeCN, **6** is much less soluble than **5** and rapidly precipitated from the solution; after filtration and washing with a 1:3 mixture of thf and Et_2O, **6** was isolated with a 55% yield. Complex **5** was recovered in 64% yield after evaporation of acetonitrile and washing with thf. Yellow crystals of **5**·MeCN were obtained by slow diffusion of diethyl ether into an acetonitrile solution, and yellow-orange crystals of **6** were deposited from a cooled acetonitrile solution. Crystals of the terpyridine analogue $[UO_2(NO_3)_2(terpy)]$ were previously obtained by slowly heating a 1:1 mixture of $UO_2(NO_3)_2·6H_2O$ and terpy in acetone.[10]

In contrast to **1** and **2**, the nitrate compounds **5** and **6** in acetonitrile exhibit broad ^{1}H NMR signals at 23 °C; the spectra became well resolved upon cooling down the solution and showed two sets of resonances corresponding to **5** or **6** and free Rbtp. These results clearly indicate that **5** and **6** are partly dissociated in solution, being in equilibrium with $[UO_2(NO_3)_2(MeCN)_n]$ and Rbtp; the thermodynamic constants relative to these equilibria were not determined because of the crystallization of the poorly soluble complexes. The distinct behavior of the analogous triflate and nitrate compounds can be easily explained by the stronger Lewis acidity of $UO_2(OTf)_2$ versus $UO_2(NO_3)_2$ and the weaker coordinating ability of the OTf versus the NO_3 ligand. This is also demonstrated by the crystal structures (vide infra) which revealed that the OTf ligands are monodentate in **1** and **2**, whereas the NO_3 groups are bidentate in **5** and **6**. That the NO_3 ligand is more tightly bound to the metal center than OTf and thus more difficult to replace is also evidenced in solution by the inertness of **5** and **6** toward an excess of Rbtp; formation of the bis-adducts analogous to **3** and **4** was not detected by ^{1}H NMR spectroscopy. In fact, displacement of a NO_3 ligand of uranyl nitrate with a neutral Lewis base is quite rare, one example being the synthesis of $[UO_2(NO_3)(bipyO_2)_2][NO_3]$ ($bipyO_2$ = 2,2′-bipyridine-*N*,*N*′-dioxide).[31]

The IR spectra of **5** and **6** exhibit the ν_{asym}(U=O) bands at 939 and 916 cm^{-1}, respectively; the rather low value of **6**, which was measured on both a powdered and a crystalline sample, is difficult to explain. These frequencies are lower than those of the triflate analogues **1** and **2**, reflecting the greater electron-donating capacity of the nitrate ligands. The bands at 1486 and 1286 cm^{-1} for **5**, and 1492 and 1286 cm^{-1} for **6**, are characteristic of coordinated NO_3 groups;[32] as

(30) Berthet, J. C.; Miquel, Y.; Iveson, P. B.; Nierlich, M.; Thuéry, P.; Madic, C.; Ephritikhine, M. *J. Chem. Soc., Dalton Trans.* **2002**, 3265.

(31) Alcock, N. W.; Roberts, M. M. *Acta Crystallogr., Sect.C* **1987**, *43*, 476.

(32) (a) Crawford, M. J.; Mayer, P. *Inorg. Chem.* **2005**, *44*, 8481. (b) Koshino, N.; Harada, M.; Nogami, M.; Morita, Y.; Kikuchi, T.; Ikeda, Y. *Inorg. Chim. Acta* **2005**, *358*, 1857.

Table 3. Comparison of the Mebtp Complexes **1** and **3** with Their Terpy Analogues

compound	U−N_c[a]/Å	U−N_l[a]/Å	Σ(X−U−X)[b]/°	max. dev.[c] /Å	rms dev.[d] /Å	$\theta_{Nc,Nl}$[e]/°	$\theta_{Nl,Nl}$[e]/°
$[UO_2(OTf)_2(Mebtp)]$ (**1**)							
molecule A	2.595(5)	2.56(3)	361.0	0.24	0.14	12.1; 11.0	20.4
molecule B	2.588(5)	2.56(2)	361.1	0.21	0.13	11.0; 14.7	25.6
$[UO_2(OTf)_2(terpy)]$[4]	2.548(4)	2.537(5)	362.6	0.32	0.15	18.2; 22.2	27.7
$[UO_2(Mebtp)_2][OTf]_2$ (**3**)							
molecule A	2.612(4)	2.559(1)	375.5	0.43	0.36	15.6; 15.3	29.0
molecule B	2.591(4)	2.571(6)	375.7	0.43	0.36	14.4; 15.3	26.3
$[UO_2(terpy)_2][OTf]_2$[4]							
molecule A	2.588(6)	2.58(2)	378.8	0.49	0.40	21.3; 19.9	39.0
molecule B	2.578(6)	2.57(1)	379.0	0.45	0.46	22.0; 20.1	40.8

[a] The U−N_c and U−N_l distances correspond to the central and lateral (average) aromatic rings of the terdentate ligand. [b] Sum of the adjacent X−U−X angles (X = O or N, coordinating atoms of the uranyl complex). [c] Maximum deviation of individual X atoms from the mean plane defined by the U and X atoms. [d] Rms deviations of the mean plane defined by the U and X atoms. [e] $\theta_{Nc,Nl}$ and $\theta_{Nl,Nl}$ are the dihedral angles between the central and lateral and the two lateral rings of the terdentate ligand.

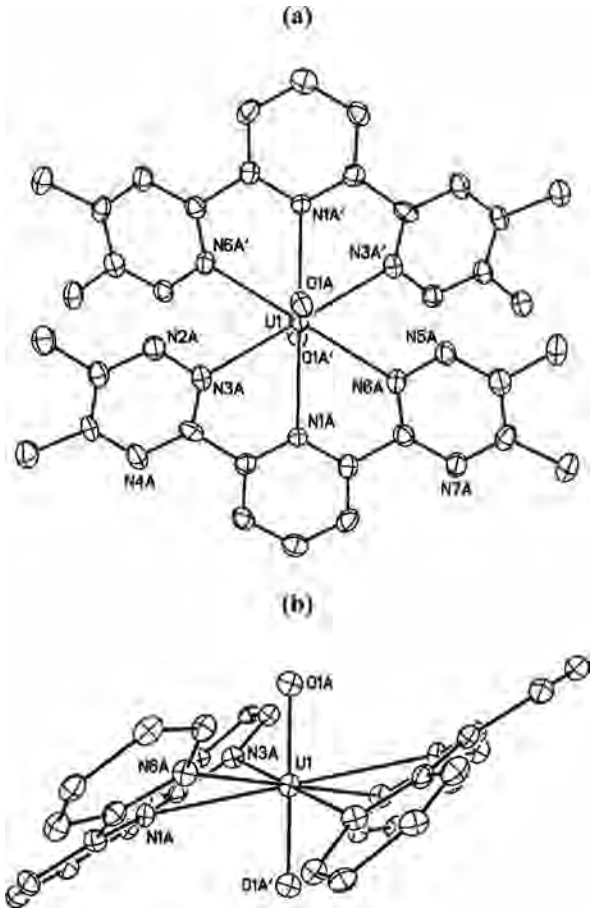

Figure 2. Views of one of the two independent cations in $[UO_2(Mebtp)_2][OTf]_2$ (**3**) along (a) and perpendicular to (b) the UO_2 axis. The hydrogen atoms have been omitted, as well as the methyl groups in b. The displacement ellipsoids are drawn at the 50% (a) or 30% (b) probability level. Symmetry code: ′ = 1 − *x*, −*y*, 2 − *z*.

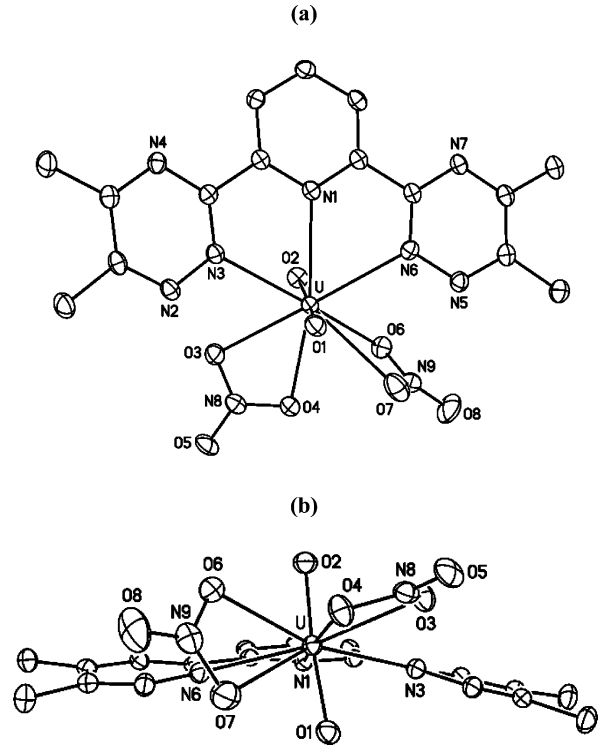

Figure 3. Views of $[UO_2(\kappa^2\text{-}NO_3)_2(Mebtp)]$ (**5**) along (a) and perpendicular to (b) the UO_2 axis. The hydrogen atoms have been omitted. The displacement ellipsoids are drawn at the 50% probability level.

previously noted, the IR spectra do not permit unambiguous identification of the coordination mode, monodentate or bidentate, of the nitrate ligand.[33a,34]

It is likely that compounds **1**−**5** are transformed in moist air into oxo and/or hydroxo derivatives, as it was previously reported with the analogous uranyl triflate or nitrate complexes with ter- or tetradente nitrogen ligands.[4,9,35a]

X-Ray Crystal Structures of $[UO_2(\kappa^2\text{-}NO_3)_2(Rbtp)]$ [R = Me (5), Pr^n (6)]. Views of the neutral complex $[UO_2(NO_3)_2(Mebtp)]$ (**5**) are represented in Figure 3a,b while selected bond distances and angles are given in Table 4. The structure, which shows the uranyl fragment surrounded by seven coordinating atoms that are three nitrogen atoms of the Mebtp molecule and four oxygen atoms of the two bidentate nitrate groups, is exceptional by its high coordination number and steric crowding. In contrast, the terpy analogue $[UO_2(NO_3)_2(terpy)]$ adopts the classical hexagonal bipyramidal configuration, one of the two nitrate ligands being in the rather rare monodentate coordination mode;[10,33] this difference would reflect the larger electron donor ability and basic character of the terpyridine molecule which facilitates the transition of the κ^2 to the κ^1 bonding mode of the NO_3 group.

Complex **5** is the second example of a seven coordinate actinyl species,[35] after the very recently reported $[UO_2(NO_3)_3(H_2O)]^-$ anion, which was found in crystals of $[(UO_2)_2$-

Table 4. Selected Distances (Å) and Angles (deg) in the Uranyl Nitrate Complexes

$[UO_2(NO_3)_2(Mebtp)]$ in **5**·MeCN	$[UO_2(NO_3)_2(Pr^nbtp)]$ (**6**)
U−O(1) 1.766(2); U−O(2) 1.770(2)	U−O(1) 1.745(3); U−O(2) 1.754(3)
U−N(1) 2.631(2); U−N(3) 2.603(2); U−N(6) 2.614(2)	U−N(1) 2.604(3); U−N(3) 2.510(3); U−N(6) 2.540(3)
U−O(3) 2.535(2); U−O(4) 2.493(2)	U−O(3A) 2.700(9); U−O(4A) 2.490(7)
U−O(6) 2.535(2); U−O(7) 2.735(3)	U−O(3B) 2.423(15)
	U−O(6) 2.567(4); U−O(7) 2.683(4)
O(1)−U−O(2) 170.49(9)	O(1)−U−O(2) 166.16(14)
O(1)−U−O(6) 116.15(8); O(1)−U−O(7) 68.48(8)	O(1)−U−O(3A) 121.7(2); O(1)−U−O(4A) 79.7(2)
O(2)−U−O(6) 73.06(8); O(2)−U−O(7) 120.87(8)	O(2)−U−O(3A) 67.7(2); O(2)−U−O(4A) 112.8(2)
	O(1)−U−O(6) 117.46(12); O(1)−U−O(7) 70.45(12)
	O(2)−U−O(6) 72.97(13); O(2)−U−O(7) 120.11(13)
N(1)−U−N(3) 60.86(7); N(1)−U−N(6) 60.74(7)	N(1)−U−N(3) 61.92(10); N(1)−U−N(6) 61.88(10)
N(3)−U−O(3) 64.18(7); N(6)−U−O(6) 67.19(7)	N(3)−U−O(3A) 74.50(17); N(3)−U−O(4A) 92.12(19)
N(6)−U−O(7) 72.14(7); O(3)−U−O(4) 50.34(7)	N(6)−U−O(6) 77.70(11); N(6)−U−O(7) 79.32(12)
O(4)−U−O(6) 65.77(7); O(4)−U−O(7) 61.79(7)	O(3A)−U−O(6) 78.51(17); O(4A)−U−O(7) 61.3(2)

$(OH)_2(terpy)_2]_2[UO_2(NO_3)_3(H_2O)][NO_3]_3 \cdot 3H_2O$.[35a] These were obtained by slow crystallization at room temperature of a 1:1 mixture of $UO_2(NO_3)_2 \cdot 6H_2O$ and terpy from acetone, but the structure could not be solved with good accuracy.[35a] A complex formulated as $[UO_2(NO_3)_2(bipyO_2)_2]$ was claimed from IR studies to contain UO_2^{2+} ions coordinated by two bidentate $bipyO_2$ ligands, one bidentate and one monodentate nitrate groups;[36] further crystallographic investigations indicated that this supposed seven coordinate uranyl complex actually exists as the six coordinate $[UO_2(NO_3)(bipyO_2)_2]^+$ ion.[31] As observed in the structure of $[UO_2(NO_3)_3(H_2O)]^-$, one of the bidentate nitrate ligands of **5**, N(9)O(6)O(7)O(8), is perpendicular to the equatorial plane of the UO_2 fragment in which the other coordinating atoms are lying. Thus, the two mean planes defined by U, N(1), N(3), N(6), O(3), O(4) and U, O(1), O(2), O(6), O(7) form a dihedral angle of 87.63(5)°; the O(6) and O(7) atoms are located on each side of the equatorial plane, at a distance of 0.833(3) and 1.303(3) Å, respectively. The greatest displacements of a coordinating atom from the equatorial plane of the UO_2^{2+} ion, 1.494(6) and 1.324(6) Å, were observed in $[UO_2(C_5Me_5)(CN)_3]^{2-}$ and $[UO_2(p\text{-}Bu^t\text{-hexahomotrioxacalix[3]arene})]^{2-}$, respectively.[37,38] The coordination geometry of **5** can be described as a distorted hexagonal bipyramid with a split equatorial vertex (Figure 4). Apart from this and the case cited above, such twisting of the planar NO_3 unit out of the equatorial plane is unprecedented in the large number of uranyl and neptunyl compounds with bidentate nitrate ligands, but it has been observed with sulfate and acetate ligands of pentavalent neptunyl compounds, where the metal environment is a pentagonal bipyramid with split vertices occupied by the oxygen atoms of the SO_4 or $MeCO_2$ groups.[39,40]

Although the structure of $[UO_2(NO_3)_3(H_2O)]^-$ was not solved with good accuracy, it appeared that the two U−O bonds of the nitrate ligand parallel to the UO_2 unit were about 0.2 Å longer than the U−O(NO_3) bonds in the equatorial plane, with average lengths of 2.71(1) and 2.54(3) Å, respectively. In complex **5**, only the U−O(7) distance of 2.735(3) Å is 0.2 Å larger than the other typical U−O(NO_3) distances which average 2.52(2) Å. We assume this nitrate to be bidentate, since in the rare uranyl complexes with monodentate nitrate ligands the single coordinating oxygen is lying in the equatorial plane, which is not the case here, and the other two oxygen atoms are generally as far as 3.38−4.51 Å from the metal atom.[10,33] The variations in the N−O distances are also in agreement with a bidentate coordination mode of the NO_3 groups. In **5**, the two N(9)−O(6) and N(9)−O(7) distances of 1.287(3) and 1.261(4) Å, respectively, are larger than the N(9)−O(8) distance of 1.209(4) Å; the geometry of the equatorial nitrate ligand N(8)O(3)O(4)O(5) is similar, the corresponding N−O distances being equal to 1.274(3), 1.274(3), and 1.210(3) Å. In contrast, monodentate nitrate ligands of uranyl complexes generally exhibit one larger N−O(U) and two smaller (UO)N−O distances.[10,33] For example, in the complex $[UO_2(\kappa^1\text{-}NO_3)(\kappa^2\text{-}NO_3)(terpy)]$,[10] the N−O bond of the monodentate nitrate with the oxygen atom included in metal coordination elongates to 1.300(7) Å, and in the bidentate nitrate, the mean length of such bonds is 1.276(7) Å; the lengths of the N−O bonds with uncoordinated oxygen atoms are identical in the monodentate and bidentate ligands, with a mean value of 1.233(7) Å.

The deviation of the UO_2 unit of **5** from the most usual linearity [170.49(9)°] is likely due to steric and electrostatic repulsions from the oxygen atoms O(6) and O(7). While more than 98% of the crystal structures of uranyl compounds

(33) (a) Graziani, R.; Marangoni, G.; Paolucci, G.; Forsellini, E. *J. Chem. Soc., Dalton Trans.* **1978**, 818. (b) Paolucci, G.; Marangoni, G.; Bandoli, G.; Clemente, D. A. *J. Chem. Soc., Dalton Trans.* **1980**, 459. (c) Bandoli, G.; Clemente, D. A.; Cingi, M. B. *J. Inorg. Nucl. Chem.* **1975**, *37*, 1709. (d) Thuéry, P.; Nierlich, M.; Vicens, J.; Masci, B.; Takemura, H. *Eur. J. Inorg. Chem.* **2001**, 637. (e) Bradley, A. E.; Hardacre, C.; Nieuwenhuyzen, M.; Pitner, W. R.; Sanders, D.; Seddon, K. R.; Thied, R. C. *Inorg. Chem.* **2004**, *43*, 2503. (f) Belomestnykh, V. I.; Sveshnikovea, L. B.; Mikhailov, Y. N.; Kanishcheva, A. S.; Gorbunova, Y. E. *Russ. J. Inorg. Chem.* **2004**, *49*, 1016.

(34) Hunter, A. P.; Lees, A. M. J.; Platt, A. W. G. *Polyhedron* **2007**, *26*, 4865.

(35) (a) Charushnikova, I. A.; Den Auwer, C. *Russ. J. Inorg. Chem.* **2007**, *33*, 53. (b) Bellad, S. B.; Babu, A. M.; Sridhar, M. A.; Indira, A.; Prasad, J. S.; Prout, K. *Mol. Cryst. Liq. Cryst. Sci. Technol., Sect. A* **1994**, *257*, 59; in this article, an eight-coordinate uranyl species, e.g., $[UO_2Cl_2(NO_3)_2(2,6Me\text{-}C_5H_3NHCOCH_2NEt_2)_2]$, is mentioned. However, the paper does not supply full crystallographic data and the atomic coordinates have not been deposited with the Cambridge Structural Database.

(36) Madan, S. K.; Chan, K. S. *J. Inorg. Nucl. Chem.* **1977**, *39*, 1007.

(37) Maynadié, J.; Berthet, J. C.; Thuéry, P.; Ephritikhine, M. *Chem. Commun.* **2007**, 486.

(38) Masci, B.; Nierlich, M.; Thuéry, P. *New J. Chem.* **2002**, *26*, 120.

(39) Grigoriev, M. S.; Barturin, N. A.; Budantseva, N. A.; Fedoseev, A. M. *Radiokhimiya* **1993**, *35*, 29.

(40) Charushnikova, I. A.; Perminov, V. P.; Katser, S. B. *Radiokhimiya* **1995**, *37*, 493.

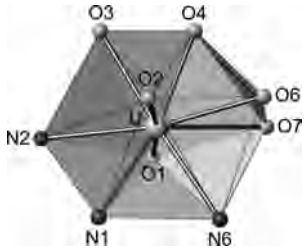

Figure 4. Coordination polyhedron in $[UO_2(\kappa^2\text{-}NO_3)_2(Mebtp)]$.

show O═U═O angles in the 174−180° range,[41,42] smaller angles have been found in $[UO_2(NO_3)_3(H_2O)]^-$ [167°(1)],[35a] $[UO_2\{(Me_3SiN)_2CPh\}_2(thf)]$ [169.7(2)°],[42] $[UO_2(C_5Me_5)(CN)_3]^{2-}$ [168.40(9)°],[37] and $[UO_2(NO_3)_2(Mebtp)]$ in **6** [166.16(14)°] (vide infra).

The crystal structure of $[UO_2(NO_3)_2(Pr^nbtp)]$ (**6**) suffers from the disorder of one of the two nitrate ligands over two positions adopting either a κ^2 or a κ^1 bonding mode, noted respectively with A and B labels; therefore, the bond lengths and angles will not be discussed in detail. This structure was determined at 200 K (instead of 100 K for the other ones), because of crystal deterioration at lower temperatures, which could be due to the occurrence of a phase transition related to the nitrate disorder. However, the structure represented in Figure 5a,b clearly shows that all the nitrate ligands are twisted out of the equatorial plane of the bent UO_2 fragment, defined by the U, N(1), N(3), and N(6) atoms (rms deviation 0.05 Å). The dihedral angles between this plane and the planar NO_3 groups containing N(8A), N(8B), and N(9) are 65.2(3), 86.7(5), and 86.09(14)°, respectively, and the displacements of the oxygen atoms out of the equatorial plane are in the range 0.526(11)−1.411(10) Å. The uranyl complex **6**, with the two bidentate NO_3 ligands, adopts a novel coordination geometry which can be described as a distorted capped square antiprism defined by the square faces O(1), O(2), N(3), N(6) (rms deviation 0.49 Å) and O(3A), O(4A), O(6), O(7) (rms deviation 0.12 Å) forming a dihedral angle of 8.86(18)°, and with N(1) in capping position (Figure 6).

Crystal Structure of $[U(CyMe_4btbp)_2(\mu\text{-}O)UO_2(\kappa^2\text{-}NO_3)_3][OTf]\cdot 2MeCN$ (7·2MeCN). In the course of our studies on the coordinating behavior of the terdentate Rbtp and tetradentate Rbtbp molecules with f-elements, we are currently investigating the affinity of such ligands for metal ions in various oxidation states. During one of these experiments, the presence of adventitious traces of air during slow diffusion of diethyl ether into an acetonitrile solution of a 1:2:1 mixture of $U(OTf)_4$, $CyMe_4btbp$, and $[UO_2(NO_3)_2(MeCN)]$ afforded few orange crystals of **7**·2MeCN. Complex **7** is a rare example of a covalently bound $[U^{IV}U^{VI}]$ mixed valence complex;[43] it is also the first complex with btbp ligands coordinated to a U(IV) ion. This complex is of particular interest in the frame of this work because the coordination number of the uranyl moiety is seven with, as in **5** and **6**, a nitrate ligand perpendicular to the equatorial plane. At this time, attempts to isolate **7** for further characterization have not been carried out, and only the crystal structure is presented. A view of the dinuclear cation is shown in Figure 7 and selected bond lengths and angles are listed in Table 5.

The nine coordinate U(1) atom is in a very distorted capped square antiprismatic environment, the square faces defined by N(1A), N(2A), N(1B), N(2B) [rms deviation 0.13 Å] and N(3A), N(4A), N(3B), N(4B) [rms deviation 0.45

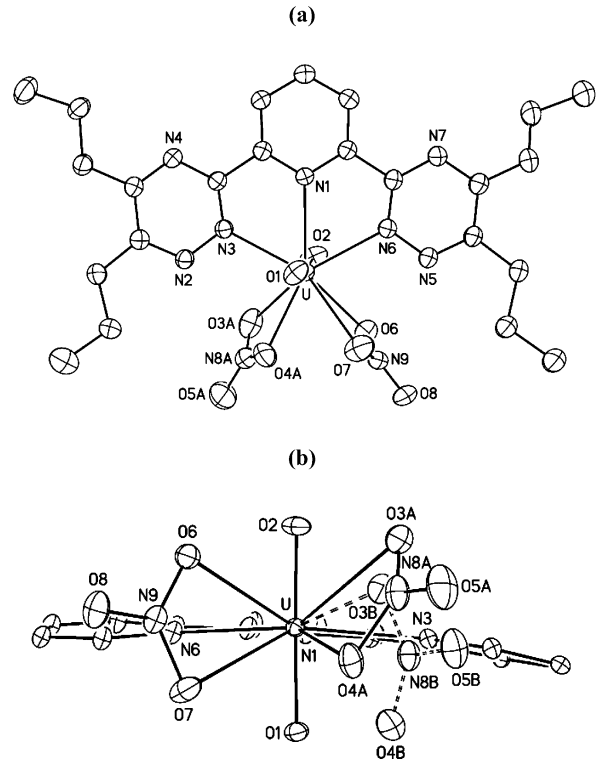

Figure 5. Views of $[UO_2(NO_3)_2(Pr^nbtp)]$ (**6**) along (a) and perpendicular to (b) the UO_2 axis. The hydrogen atoms have been omitted as well as the propyl groups in b. Only the bidentate form of the disordered nitrate ligand is represented in (a), while the two, mono- and bidentate forms are represented in (b). The displacement ellipsoids are drawn at the 30% (a) or 10% (b) probability level.

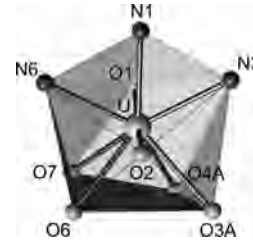

Figure 6. Coordination polyhedron in $[UO_2(NO_3)_2(Pr^nbtp)]$.

(41) Gutowski, K. E.; Bridges, N. J.; Rogers, R. D. In *The Chemistry of the Actinide and Transactinide Elements*, 3rd ed.; Morss, L. R., Edelstein, N., Fuger, J., Katz, J. J., Eds.; Springer: Dordrecht, The Netherlands, 2006; Vol. 4, Chapter 22, p 2380.

(42) Sarsfield, M. J.; Helliwell, M. *J. Am. Chem. Soc.* **2004**, *126*, 1036.

(43) (a) Allen, S.; Barlow, S.; Halasyamani, P. S.; Mosselmans, J. F. W.; O'Hare, D.; Walker, S. M.; Walton, R. I. *Inorg. Chem.* **2000**, *39*, 3791. (b) Wang, C. M.; Liao, C. H.; Lin, H. M.; Lii, K. H. *Inorg. Chem.* **2004**, *43*, 8239; and references therein. (c) Bombieri, G.; Benetollo, F.; Kläne, E.; Fischer, R. D. *J. Chem. Soc., Dalton Trans.* **1983**, 115. (d) Beeckman, W.; Goffart, J.; Rebizant, J.; Spirlet, M. R. *J. Organomet. Chem.* **1986**, *307*, 23.

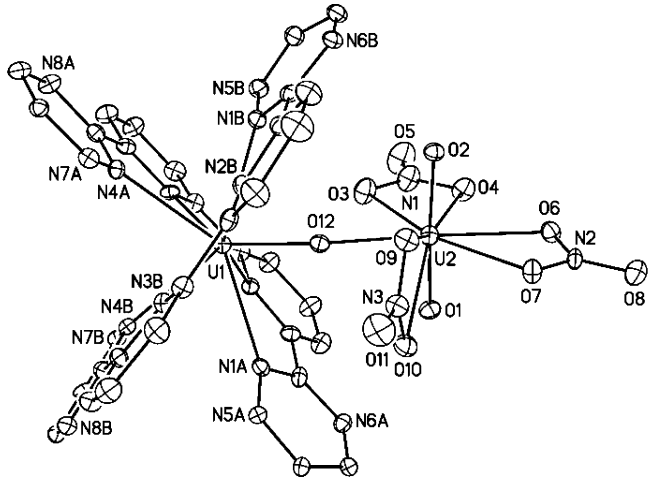

Figure 7. View of the cation $[U(CyMe_4btbp)_2(\mu\text{-}O)UO_2(\kappa^2\text{-}NO_3)_3]^+$ in (**7**). The hydrogen atoms and the tetramethylcyclohexyl groups have been omitted. The displacement ellipsoids are drawn at the 20% probability level.

Å] forming a dihedral angle of 1.67(2)°, and the bridging atom O(12) in capping position. The average U−N distance of 2.59(2) Å can be compared with those of 2.51(3)−2.60(2) Å measured in a series of $[UO_2X_2(CyMe_4btbp)]$ compounds.[9] In these uranyl complexes, the uranium atom lies in the plane of the tetradentate ligand, which occupies the equatorial girdle of the UO_2^{2+} ion, and the U−N_c distances with the central bipyridyl groups are about 0.05 Å larger than the U−N_l distances with the lateral triazine rings, suggesting that the approach of the metal center toward the N_c atoms in the equatorial plane is impeded by its coordination to the N_l atoms. In contrast, the U(1) atom in **7** is at about 0.7 Å from the two planar btbp ligands, which form a dihedral angle of 73.60(3)°, and the U−N_c distances are then about 0.05 Å smaller than the U−N_l distances.

The two uranium atoms are bridged by the μ-oxo atom O(12) in an asymmetric fashion while the U(1)–O(12)−U(2) angle is close to linearity (172.0(3)°). This difference between the U−O bonds is opposite to that expected from the variation in the oxidation numbers of U(1) and U(2), which are both nine coordinate, because the radius of the U(IV) ion is about 0.15 Å larger than that of U(VI).[44] Such asymmetry in oxo bridges, which has been encountered in the structures of the dinuclear uranium(IV) compound $[(18\text{-crown-6})(BH_4)U(\mu\text{-}O)U(BH_4)_5]$ [U−O = 1.979(5) and 2.187(5) Å][45] and of some polynuclear uranyl complexes exhibiting the so-called cation−cation interactions, like $[(UO_2)_4(\mu\text{-}O)_2(SC_5NH_4)_6]^{2-}$ [U−O(μ-oxo) = 1.838(7) and 2.488(7) Å][46] or $[UO_2\{O(CHPr^i)_2\}_2]_4$ [U−O(μ-oxo) = 1.846(4) and 2.435(4) Å],[47] have been accounted for by the major contribution of the U=O→U bonding scheme to the true structure of the oxo bridge. The distinct U(1)−O(12) and U(2)−O(12) distances of 1.964(6) and 2.240(6) Å in **7** are thus likely indicative of a U(1)=O(12)→U(2) dative interaction, associated with the dicationic $[U(CyMe_4\text{-}btbp)_2(=O)]^{2+}$ and anionic $[UO_2(NO_3)_3]^-$ species. The U(1)−O(12) distance is larger than those found in uranium(IV) oxo compounds, which vary from 1.860(3) Å in $[U(C_5H_2Bu^t_3)_2(O)(4\text{-}Me_2NC_5H_4N)]$[48] to 1.917(6) Å in $[U(Cp^*)_2(O)(C\{NMeCMe\}_2)]$.[49] The U(2)−O(12) bond is shorter than the UO dative bond in the uranyl complexes $[UO_2(NO_3)_3(H_2O)]^-$ [U−O(H_2O) = 2.38(1) Å],[16] $[UO_2(NO_3)_2(H_2O)_2]$ [U−O(H_2O) = 2.397(3) Å],[50] or $[UO_2(NO_3)_2(pinacol)]$ [U−O(pinacol) = 2.445(4) and 2.452(4) Å].[51]

The uranyl moiety in **7** adopts the same coordination geometry as **5** and $[UO_2(\kappa^2\text{-}NO_3)_3(H_2O)]^-$. The planar $N(3)O_3$ group forms a dihedral angle of 87.4(3)° with the equatorial plane defined by the U(2), O(3), O(4), O(6), O(7), O(12) atoms [rms deviation 0.04 Å], and the O(9) and O(10) atoms are located on each side of this plane, at a distance of 1.003(9) and 1.143(9) Å, respectively. Repulsive interactions induced by these latter oxygen atoms cause the O(1)−U(2)−O(2) angle to deviate from linearity by 9.6(3)°. The two nitrate ligands lying in the equatorial girdle are in relative cis positions whereas they are in trans configuration in the aquo derivative.

The U(2)−O(10) bond is 0.27 Å longer than the U(2)−O(9) bond which is similar to the equatorial U−O(NO_3) bonds. This feature, also observed in **5**, as well as the fact that one nitrate ligand of **6** adopts either a mono- or a bidentate ligation mode, strongly suggests that the κ^2-to-κ^1 transition of the NO_3 group perpendicular to the equatorial plane is a facile process. According to recent Car−Parrinello molecular dynamics simulations, the κ^2 coordination in $[UO_2(NO_3)_3]^{2-}$ is clearly favored in the gas phase and in solution, while solvation effects facilitate the transition of one chelating nitrate ligand of $[UO_2(NO_3)_2(H_2O)]$ to a κ^1 bonding mode.[52,53] Such simulations also revealed that $[UO_2(\kappa^2\text{-}NO_3)_2(H_2O)(\kappa^1\text{-tmma})]$ (tmma = $Me_2NCOCH_2CONMe_2$) could be transformed into $[UO_2(\kappa^2\text{-}NO_3)(\kappa^1\text{-}NO_3)(H_2O)(\kappa^2\text{-tmma})]$ in water, and that the κ^1 nitrate is quite mobile and readily rotates around the U−O bond, affording instantaneous structures where the NO_3 plane is aligned parallel with the uranyl axis. However, the κ^2 coordination of this NO_3 ligand out of the equatorial plane and the formation of seven coordinate uranyl species were not predicted.

Density Functional Theory Analysis of the $[UO_2(NO_3)_2(L)]$ (L = Mebtp, terpy) Complexes. We provide molecular orbital calculations at the DFT level to try to explain the above observations, that is, the difference in the coordination mode in the $[UO_2(NO_3)_2(L)]$ (L = Mebtp, terpy) complexes. We supply a qualitative picture of the interaction (orbital, charge transfer, energy) in these complexes. The main

(44) Shannon, R. D. *Acta Crystallogr., Sect. A* **1976**, *32*, 751.
(45) Villiers, C.; Thuéry, P.; Ephritikhine, M. *Acta Crystallogr., Sect.C* **2006**, *62*, m243.
(46) Rose, D.; Chang, Y. D.; Chen, Q.; Zubieta, J. *Inorg. Chem.* **1994**, *33*, 5167.
(47) Wilkerson, M. P.; Burns, C. J.; Dewey, H. J.; Martin, J. M.; Morris, D. E.; Paine, R. T.; Scott, B. L. *Inorg. Chem.* **2000**, *39*, 5277.
(48) Zi, G.; Jia, L.; Werkema, E. L.; Walter, M. D.; Gottfriedsen, J. P.; Andersen, R. A. *Organometallics* **2005**, *24*, 4251.
(49) Evans, W. J.; Kozimor, S. A.; Ziller, J. W. *Polyhedron* **2004**, *23*, 2689.
(50) Taylor, J. C.; Mueller, M. H. *Acta Crystallogr.* **1965**, *19*, 536.
(51) Villiers, C.; Thuéry, P.; Ephritikhine, M. *Polyhedron* **2004**, *23*, 1613.
(52) Bühl, M.; Kabrede, H.; Diss, R.; Wipff, G. *J. Am. Chem. Soc.* **2006**, *128*, 6357.
(53) Bühl, M.; Diss, R.; Wipff, G. *Inorg. Chem.* **2007**, *46*, 5196.

Table 5. Selected Distances (Å) and Angles (deg) in the $[U^{IV}U^{VI}]$ Mixed Valence Complex $[U(CyMe_4btbp)_2(\mu\text{-}O)UO_2(\kappa^2\text{-}NO_3)_3][OTf]$

around U(1)[a]	around U(2)
U(1)−N(1A) 2.621(7) [2.626(7)]	U(2)−O(1) 1.761(6); U(2)−O(2) 1.776(6)
U(1)−N(2A) 2.569(6) [2.574(7)]	U(2)−O(3) 2.552(7); U(2)−O(4) 2.579(6)
U(1)−N(3A) 2.580(6) [2.565(6)]	U(2)−O(6) 2.562(7); U(2)−O(7) 2.519(6)
U(1)−N(4A) 2.616(7) [2.606(7)]	U(2)−O(9) 2.569(6); U(2)−O(10) 2.836(7)
U(1)−O(12) 1.964(6)	U(2)−O(12) 2.240(6)
N(1A)−U(1)−N(2A) 62.2(2) [62.8(2)]	O(1)−U(2)−O(2) 170.4(3); O(1)−U(2)−O(9) 116.5(2)
N(2A)−U(1)−N(3A) 62.4(2) [63.1(2)]	O(1)−U(2)−O(10) 69.8(2); O(2)−U(2)−O(9) 73.0(2)
N(3A)−U(1)−N(4A) 62.8(2) [62.6(2)]	O(2)−U(2)−O(10) 119.6(2); O(3)−U(2)−O(4) 49.3(2)
N(1A)−U(1)−O(12) 73.6(2) [74.0(2)]	O(4)−U(2)−O(6) 60.6(2); O(6)−U(2)−O(7) 50.31(19)
N(2A)−U(1)−O(12) 81.3(2) [76.9(2)]	O(7)−U(2)−O(9) 65.7(2); O(7)−U(2)−O(10) 64.7(2)
N(3A)−U(1)−O(12) 119.8(2) [111.6(2)]	O(3)−U(2)−O(12) 67.2(2); O(9)−U(2)−O(12) 71.4(2)
N(4A)−U(1)−O(12) 141.2(2) [139.7(2)]	O(10)−U(2)−O(12) 71.8(2)

[a] The corresponding values in the ligand labeled B are given in square brackets.

calculations were performed in the ADF framework that is well established and recognized for giving accurate results.[54–58] The related theoretical methods are outlined in the Experimental Section.

Molecular Geometry Optimization. Different conformers were built starting from the crystal structure and varying the bonding mode of the nitrate groups (κ^1 or κ^2) or their positions parallel (//) or perpendicular ($\perp$) to the uranyl equatorial plane. A vibrational frequency calculation was performed for each optimized geometry to confirm the convergence to minima on the potential energy surface. In these compounds, various orientations of the nitrate groups can correspond to local minima with similar energies. Our goal is not to perform an exhaustive potential energy surface exploration but rather to probe some characteristic conformations.

For the Mebtp and terpy uranyl complexes, the most energetically stable structure is obtained with one bidentate nitrate ligand in the equatorial plane and the other perpendicular to this plane (see Supporting Information for the optimized coordinates). However, the bonding mode for this axial NO_3 group is κ^2 in the Mebtp complex and κ^1 in the terpyridine analogue. A geometry with two bidendate nitrate ligands perpendicular to the equatorial plane of the uranyl fragment is found higher in energy, by about 6 kJ mol^{-1} for the Mebtp compound and 17 kJ mol^{-1} for the terpy derivative (MP2 calculations). This conformation could be energetically accessible for other Rbtp complexes as observed in the crystal structure of the propyl derivative **6**. The structure with two bidentate nitrate groups in the equatorial plane is about 17 kJ mol^{-1} higher for Mebtp (MP2 calculations) and then not viable. Finally, the most stable geometry of the Mebtp complex **5**, with the uranyl fragment surrounded by seven coordinating atoms, is confirmed by theoretical calculations; in contrast, such a geometry is not obtained with the terpyridine counterpart, a fact that can be mainly explained by the greater electrostatic repulsions. The deviation of the UO_2^{2+} unit from linearity is pronounced when the NO_3 group perpendicular to the equatorial plane adopts the η^2 ligation mode, in agreement with the crystal structure.

Table 6. Optimized DFT Distances (Å) and Angles (deg) in the Uranyl Nitrate Complexes $[UO_2(\kappa^2\text{-}NO_3)_2(Mebtp)]$ and $[UO_2(\kappa^2\text{-}NO_3)(\kappa^1\text{-}NO_3)(terpy)]$[a]

$[UO_2(NO_3)_2(Mebtp)]$	$[UO_2(NO_3)_2(terpy)]$
U−O(1) 1.796; U−O(2) 1.804	U−O(1) 1.794; U−O(2) 1.795
U−N(1) 2.750; U−N(3) 2.663; U−N(6) 2.692	U−N(1) 2.726; U−N(3) 2.705; U−N(6) 2.676
U−O(3) 2.541; U−O(4) 2.508	U−O(3) 2.519; U−O(4) 2.499
U−O(6) 2.480; U−O(7) 2.718	U−O(6) 3.603; U−O(7) 2.336
O(1)−U−O(2) 163.1	O(1)−U−O(2) 173.3

[a] The atom labelling is identical to that in the crystal structures.

Table 7. Energy Decomposition (kJ mol^{-1}) for the Uranyl Nitrate Complexes $[UO_2(\kappa^2\text{-}NO_3)_2(Mebtp)]$ and $[UO_2(\kappa^2\text{-}NO_3)(\kappa^1\text{-}NO_3)(terpy)]$

	$[UO_2(NO_3)_2(Mebtp)]$	$[UO_2(NO_3)_2(terpy)]$
Pauli repulsion	965.67	1001.87
electrostatic interaction	−2466.37	−2487.26
total steric interaction	−1500.70	−1485.39
orbital interactions	−885.36	−919.49
total bonding energy	−2386.06	−2404.88

The DFT optimized geometries obtained for the Mebtp and terpy uranyl complexes are in good agreement with the experimental structures. The bond lengths are generally overestimated by 0.03−0.06 Å with a maximum deviation of 0.17 Å for one U−N distance in the terpy compound (Table 6). The bent uranyl structure and the bonding mode of the NO_3 groups are also well reproduced by the DFT calculations.

All the theoretical results and discussions in the following are related to the most energetically stable structure.

Electronic Structure and Bond Energy Decomposition. The energy decomposition analysis results are summarized in Table 7. The bonding energy is more negative for the terpy than for the Mebtp compound. A large part of the negative total bonding energy for the two compounds results from the electrostatic interaction. Closer analysis shows that the steric interaction (Pauli repulsion + electrostatic interaction) is slightly larger in the Mebtp than in the terpy complex by 15 kJ mol^{-1}. The orbital interaction is significantly more negative for the terpy than for the Mebtp compound, resulting in the greater stability of the former by 34 kJ mol^{-1}. The origin of this difference, which is quite difficult to establish in these large systems without any symmetry elements, is chemically in agreement with the greater Lewis base properties of terpy. However, there is clearly a difference in the nature of the orbitals associated

(54) Häller, L. J. L.; Kaltsoyannis, N.; Sarsfield, M. J.; May, I.; Cornet, S. M.; Redmond, M. P.; Helliwell, M. *Inorg. Chem.* **2007**, *46*, 4868.
(55) Krapp, A.; Bickelhaupt, F. M.; Frenking, G. *Chem.—Eur. J.* **2006**, *12*, 9196.
(56) Lein, M.; Szabó, A.; Kovács, A.; Frenking, G. *Faraday Discuss.* **2003**, *124*, 365.
(57) Patzschke, M.; Pyykkö, P. *Chem. Commun.* **2004**, 1982.
(58) Dognon, J. P.; Clavaguéra, C.; Pyykkö, P. *Angew. Chem., Int. Ed.* **2007**, *46*, 1427.

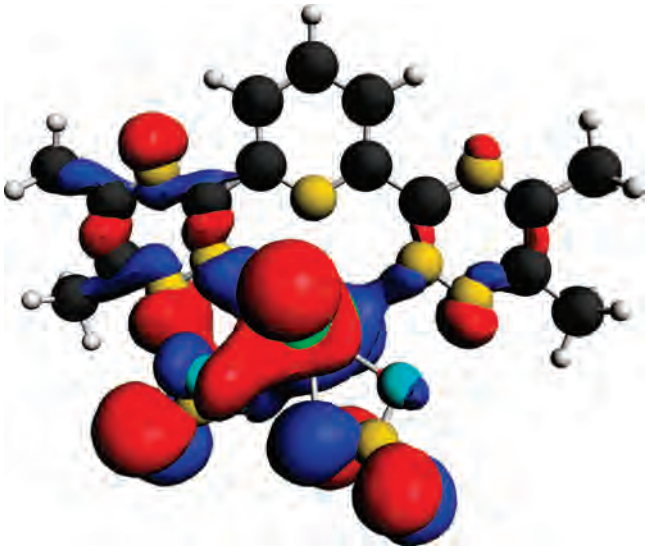

Figure 8. Molecular orbital HOMO−4 involving the NO_3^-, UO_2^{2+}, and Mebtp moieties in $[UO_2(NO_3)_2(Mebtp)]$.

Table 8. Voronoi Deformation Density (VDD) for the Uranyl Nitrate Complexes $[UO_2(\kappa^2\text{-}NO_3)_2(Mebtp)]$ and $[UO_2(\kappa^2\text{-}NO_3)(\kappa^1\text{-}NO_3)(terpy)]$

	$[UO_2(NO_3)_2(Mebtp)]$	$[UO_2(NO_3)_2(terpy)]$
$\{UO_2\}^{2+}$	−0.610	−0.584
NO_3^- (//)	0.226	0.221
NO_3^- (⊥)	0.268	0.225
nitrogen ligand	0.117	0.138

to the bonding interaction for the two systems. In each compound, one of the main orbital interactions is between the nitrate ligand and the uranyl group. The highest occupied molecular orbital (HOMO) to HOMO−2 in the Mebtp complex and HOMO to HOMO−11 (see Supporting Information for the visualization of these orbitals) in the terpy derivative contribute to these interactions with a participation of the uranium 5f orbital varying from 0% to 13%. In the Mebtp complex, an orbital interaction among the UO_2^{2+}, NO_3^-, and Mebtp moieties is found. This is particularly well illustrated with the example of the HOMO−4 molecular orbital, represented in Figure 8, which is essentially associated with an orbital interaction between the O(2p) orbital from the nitrate group perpendicular to the equatorial plane (19%), the U(5f) (16%), O_{yl}(2p) (17%) orbitals from the uranyl group and the N(2p) (11%) orbital from the triazine rings. We can also note the unexpected orbital participation of the nitrogen atom adjacent to the nitrogen coordinating atom of the lateral triazine rings of the Mebtp ligand. The situation is quite distinct in the terpyridine complex where the bonding is essentially between the UO_2^{2+} and NO_3^- or the UO_2^{2+} and terpy units. It is noteworthy that the more planar geometry of Mebtp versus that of terpy could also be related to these orbital interactions between the uranyl unit and the nitrate and terdentate nitrogen ligands.

The Voronoi Deformation Density (VDD) analysis (Table 8) reveals a charge transfer to the uranyl of −0.610 and −0.584 e in the Mebtp and terpy compounds, respectively. This electron transfer is mainly provided by the nitrate groups, in particular the κ^2-NO_3^- (⊥) which exhibits the greater donation, but also, to a lesser extent, by the nitrogen ligands with a charge transfer slightly larger in the terpyridine compound. These results are supported by the Mayer Bond Order (MBO) analysis presented in Table 9. The MBOs of the U−N bonds are slightly smaller in the Mebtp than in the terpy complex; the opposite trend is observed for the MBOs of the U−O_{yl} and the U−O(NO_3) bonds. These results are in agreement with the stronger electron donating effect of the terpy versus Mebtp ligand. The greater negative charge transferred by terpy onto the uranyl moiety would be compensated by a lesser electron donation of the nitrate anions, as observed in the case of the monodentate coordination mode of the axial nitrate in $[UO_2(NO_3)_2(terpy)]$.

Table 9. Mayer Bond Orders of the Bonds to Uranium in the $[UO_2(\kappa^2\text{-}NO_3)_2(Mebtp)]$ and $[UO_2(\kappa^2\text{-}NO_3)(\kappa^1\text{-}NO_3)(terpy)]$ Complexes

	$[UO_2(NO_3)_2(Mebtp)]$	$[UO_2(NO_3)_2(terpy)]$
U−O_{yl}	2.065	2.045
U−O (nitrate //)	0.388	0.377
	0.395	0.385
U−O (nitrate ⊥)	0.413	0.546
	0.388	
U−N (central)	0.187	0.211
U−N (lateral)	0.206	0.237
	0.202	0.243

Another consequence of the strong interaction between the nitrate ligand perpendicular to the equatorial plane and the uranyl group is the bending of the O_{yl}−U−O_{yl} fragment, that one can expect as a result of the strong electrostatic repulsion between negatively charged oxygen atoms from this NO_3 group (maximized in the κ^2 mode) and the uranyl unit.

Conclusion

Addition of the terdentate ligand Rbtp to $UO_2(OTf)_2$ led to the complexes $[UO_2(OTf)_2(Rbtp)]$ and $[UO_2(Rbtp)_2][OTf]_2$ (R = Me, Pr^n) whose crystal structures are similar to those of their terpy analogues, providing a new uranyl compound in the unusual rhombohedral configuration. In contrast to terpy which gave with $UO_2(NO_3)_2$ the classical hexagonal bipyramidal complex $[UO_2(NO_3)_2(terpy)]$, treatment of the uranyl nitrate with Rbtp (R= Me, Pr^n) afforded seven-coordinate uranyl compounds exhibiting an extremely rare coordination geometry with the bidentate nitrate ligand twisted out of the equatorial plane. Theoretical calculations confirm the great stability of $[UO_2(\kappa^2\text{-}NO_3)_2(Mebtp)]$ with both bidentate equatorial and axial nitrate groups while $[UO_2(NO_3)_2(terpy)]$ has energy minima with a monodentate axial nitrate group. The terpyridine complex is more stabilized than its Mebtp counterpart by orbital interactions, and most of the electron density transferred to the uranyl moiety is provided by the nitrate groups in the two complexes. The axial NO_3^- anions favor strong charge transfer, in particular the bidentate group which also induces the bending of the uranyl fragment by repulsive electrostatic interactions. These calculations, which are in full agreement with the experimental observations, establish the pre-eminent role of the coordinating nitrate anions in the stability and the geometry of the complexes and afford crucial information on the electronic effect of the axial nitrate groups. The peculiar bidentate ligation mode of the axial nitrate ligand was also found in the $[U^{IV}U^{VI}]$ mixed valence complex $[U(CyMe_4\text{-}btbp)_2(\mu\text{-}O)UO_2(NO_3)_3][OTf]$. Although the crystal structures

could result at least in part from a "solid state" effect, they also suggest that such coordination of the nitrate ligand could be involved in the transition of the κ^2 to the κ^1 bonding mode of the NO_3 group, which has a large influence on the complexation and extraction processes of actinyl nitrates with organic solvents and molecules. Finally, it could be interesting in future work to change the triflate and nitrate groups with a less electron withdrawing but as bulky a ligand such as the bidentate carboxylate RCO_2^- to investigate the electronic impact and the influence of the R substituent on the structure of the products.

Acknowledgment. We are grateful to the French Group of Researches PARIS and the Direction of Nuclear Energy (DEN-DSOE) of the Commissariat à l'Energie Atomique for their financial support. We also thank Drs. C. Hill (CEA) and A. Geist (ITU) for samples of Pr^{n}btp and Dr. M. R. StJ. Foreman (University of Reading) for a sample of $CyMe_4$btbp, which were supplied in the frame of the Nuclear Fission Safety Program of the European Union under the EURO-PART contract number FI6W-CT-2003-508854.

Note Added in Proof: During the submission of this paper, the diglycolamide complex $[UO_2(NO_3)_2(DGA)]$ was reported in which one of the two nitrate ligands is coordinated in an unusual quasi-bidentate mode that is oriented parallel to the dioxo group, see Kannan, S; Moody, M. A.; Barnes, C. L.; Duval, P. B. *Inorg. Chem.* **2008**, *47*, 4691.

Supporting Information Available: Tables of crystal data, atomic positions and displacement parameters, anisotropic displacement parameters, bond lengths and bond angles in CIF format. DFT optimized coordinates, HOMO to HOMO-11 orbitals. This material is available free of charge via the Internet at http://pubs.acs.org.

IC8004486